

MASS SPECTROMETER MEASUREMENTS OF TEST GAS

68024

COMPOSITION IN A SHOCK TUNNEL

P-9

K.A. Skinner\* and R.J. Stalker†

Department of Mechanical Engineering, University of Queensland

INTRODUCTION

AGI

Shock tunnels afford a means of generating hypersonic flow at high stagnation enthalpies, but they have the disadvantage that thermochemical effects make the composition of the test flow different to that of ambient air. The composition can be predicted by numerical calculations of the nozzle flow expansion, using simplified thermochemical models and, in the absence of experimental measurements, it has been necessary to accept the results given by these calculations.

This note reports measurements of test gas composition, at stagnation enthalpies up to  $12.5 \text{ MJ.kg}^{-1}$ , taken with a time-of-flight mass spectrometer. Limited results have been obtained in previous measurements<sup>(1)</sup>. These were taken at higher stagnation enthalpies, and used a quadruple mass spectrometer. The time-of-flight method was preferred here because it enabled a number of complete mass spectra to be obtained in each test, and because it gives good mass resolution over the range of interest with air (up to 50 a.m.a.)

EXPERIMENTS

The experiments were conducted in the free piston shock tunnel T4 at the University of

---

\* Postgraduate Student

† Emeritus Professor of Space Engineering, Associate Fellow AIAA  
Department of Mechanical Engineering  
University of Queensland  
Brisbane 4072  
AUSTRALIA

Queensland<sup>(2)</sup>, using a helium-argon mixture as driver gas. The shock tube, of 10 m length and 75 mm diameter, was operated in the shock reflected mode, and supplied shock heated air to a contoured hypersonic nozzle with a throat diameter of 25.4 mm, and an exit diameter of 261 mm. As shown in fig 1(a), the mass spectrometer sampled the flow from a point on the nozzle centreline, well within the test cone of the nozzle flow field.

The stagnation enthalpy was calculated for equilibrium air from the shock speed and initial shock tube filling pressure, with an isentropic expansion to the measured nozzle reservoir pressure of  $14.0 \pm 2.5$  MPa. The estimated accuracy of the stagnation enthalpy was from +4% to -8%. To avoid problems with driver gas contamination of the test flow, the test time was confined to a period from 0.5 to 1.0 milliseconds after initiation of flow in the test section, and the stagnation enthalpy was limited to  $12.5 \text{ MJ.kg}^{-1}$ .

The mass spectrometer is described in ref.3. Essentially, it sampled the flow through a series of three conical skimmers to form a molecular beam. This was bombarded by a 250 e.V. electron beam for 200 nanoseconds every 55 microseconds, and each time a pulse of ions was produced which passed into the 1 m long drift tube, and hence to an electron multiplier detector at the end of the tube. Since the time of arrival of the ions depended on their mass, a mass spectrum of the type shown in figs 1(b) and 1(c) was obtained every 55 microseconds, and was recorded by a 50 MHz digital oscilloscope.

Peaks of  $\text{N}_2$ ,  $\text{O}_2$ , N and O are evident in the spectrum of fig 1(b), as well as some residual  $\text{H}_2\text{O}$ . The area under each peak is proportional to the number of particles of that particular mass to reach the detector. There is clearly a problem with overlap of the peaks of  $\text{N}_2$ , NO and  $\text{O}_2$ , and this particularly effects measurement of the NO peaks. Therefore some tests were made in which fewer spectra were taken, but the sampling rate of the oscilloscope was increased. The resolution was therefore improved, as shown in fig 1(c), and these spectra were used for measurements of the NO peak.

## RESULTS AND DISCUSSION

The ratio of the measurements of peak sizes is presented in fig. 2 for  $O_2/N_2$ ,  $NO/N_2$  and  $O/O_2$ . Each of the points plotted is the mean of a number of readings during a test, and therefore may be regarded as the mean of a statistical sample. The error bars indicate the standard deviation of that mean.

The measurements are compared with theoretical curves for the relative peak sizes. These were obtained by first performing numerical calculations<sup>(4)</sup> of the inviscid nonequilibrium steady expansion through the shock tunnel nozzle to yield the freestream species concentrations. These were then used to obtain values for the relative size of the mass spectra peaks. The effect of mass separation in the molecular beam was assessed by testing in the shock tunnel with known mixtures of nitrogen and helium, and nitrogen and argon. This indicated that the relative enhancement of the molecular species considered was less than 10%. The relative number of ions produced was determined from the ionization cross-sections given in table 1, and the relative efficiency with which ions were collected was taken as unity. This was checked by operating the instrument "ex tunnel" (ie. outside the shock tunnel), with the first of the three skimmers replaced by a solenoid valve, which delivered a short pulse of room air to the mass spectrometer. The measured ratio of the  $O_2$  peak area to  $N_2$  peak area was  $0.30 \pm 0.02$  which, allowing for the uncertainty in ionization cross sections, compared satisfactorily with the expected value of 0.25.

**Table 1. Electron Impact Ionization Cross-Sections at 250 e.V.**

Process	Cross-Section (cm <sup>2</sup> )	Error (%)	Reference
$O_2 + e \rightarrow O_2^+ + 2e$	$1.57 \times 10^{-16}$	13	5
$O + e \rightarrow O^+ + 2e$	$1.08 \times 10^{-16}$	5	6
$N_2 + e \rightarrow N_2^+ + 2e$	$1.68 \times 10^{-16}$	8	7
$NO + e \rightarrow NO^+ + 2e$	$1.89 \times 10^{-16}$	20	8

To calculate theoretical values for the peaks of atomic oxygen, the combined effect of mass separation and ion collection efficiency was obtained from the helium/nitrogen and nitrogen/argon results by assuming that these effects varied linearly with the mass ratio of the two species, yielding a factor of  $2.0 \pm 0.4$  for enhancement of O with respect to  $O_2$ . This was applied to the predicted numerical values for relative concentrations of O and  $O_2$  and, taking account of the ionization cross-sections, the theoretical curve in fig. 2(c) was obtained. Because of uncertainties in mass separation and ion collection efficiencies, as well as in ionization cross-sections, a possible error attaches to all the theoretical curves. The limits of this are indicated by the broken lines on either side of each curve.

It will be noted that the effect of dissociative ionization of the  $O_2$  molecule in the mass spectrometer, with production of ionized O atoms, has not been taken into account in obtaining the theoretical curve of fig. 2(c). This is because the experimental results in the tunnel show the ratio of peak sizes increasing with enthalpy from a value near zero, and this is not consistent with the presence of a substantial number of O ions due to dissociative ionization. On the other hand, it must be observed that results of the "ex tunnel" tests shown in fig. 2(c) demonstrate that substantial dissociative ionization does indeed take place in air which is supplied from a room temperature source. It may be speculated that this difference is due to thermal excitation of the  $O_2$  molecules in the tunnel flow, leading to an increased velocity spread and consequent lowered collection efficiency of the O ions resulting from dissociative ionization. However, until this apparent anomaly is resolved, some doubt must attach to the experimental results of fig. 2(c). Therefore, notwithstanding the remark made below concerning their validity, their worth is mainly in indicating the stagnation enthalpy at which the rise in O atom concentration due to free stream dissociation takes place.

The overall ratio of the number of atoms of oxygen in any form to nitrogen in any form can be obtained from the results in fig. 2. If the "ex tunnel" result in fig. 2(a) is used to generate a calibration factor for the  $O_2/N_2$  ratio, values of  $0.33 \pm 0.04$ ,  $0.27 \pm 0.03$  and  $0.30 \pm 0.04$  are obtained

for the overall ratio at stagnation enthalpies of  $8.3 \text{ MJ kg}^{-1}$ ,  $10 \text{ MJ kg}^{-1}$  and  $12.5 \text{ MJ kg}^{-1}$  respectively. The expected value is  $0.27 \pm 0.05$ , the quoted error limits resulting from residual uncertainties in the ionization cross-sections, together with the mass separation and ion collection efficiencies, after the calibration for the  $\text{O}_2/\text{N}_2$  ratio has been taken into account. Thus, the values for the overall oxygen/nitrogen ratio fall within the quoted limits of error, and provide confirmation of the experimental measurements.

It is worth remarking that, at  $12.5 \text{ MJ.kg}^{-1}$ , the measured  $\text{O}/\text{O}_2$  value in fig. 2(c) contributes a substantial 0.08 of the total oxygen/nitrogen ratio of 0.30, thereby providing an indirect confirmation of the  $\text{O}/\text{O}_2$  measurement.

It can be seen that the experimental measurements in fig. 2 generally fall outside the theoretical limits indicated by the broken lines. In fig. 2(a) the proportion of molecular oxygen exceeds theoretical limits as the stagnation enthalpy is increased. This is consistent with the results in fig. 2(c), which shows the proportion of atomic oxygen remaining at low levels for much higher enthalpies than predicted. The proportion of nitric oxide is shown in fig. 2(b), and is seen to be in excess of predicted values, at least for the range of stagnation enthalpies covered by the results. The numerical model<sup>(4)</sup> on which the theoretical curves are based gives free stream compositions which are consistent with those given by other numerical models<sup>(9)</sup>. Therefore, even when allowance is made for the experimental uncertainties, there are clear discrepancies between the theory of non-equilibrium nozzle flow and the results of these experiments, indicating a need for further experimental and theoretical work. Until these discrepancies are resolved predictions of the composition of test section flows in high enthalpy facilities should be treated with caution.

### Acknowledgments

The authors gratefully acknowledge the support received from the Australian Research Council and through NASA grant NAGW-674.

REFERENCES

1. Crane, K.C.A., and Stalker, R.J, "Mass-spectrometric Analysis of Hypersonic Flows" J. Phys. D: Appl. Phys., Vol 10, 1977, pp 679-695.
2. Stalker, R.J., "Recent Developments with Free Piston Drivers". Proceedings of the 17<sup>th</sup> Int. Symp. on Shock Waves & Shock Tubes. AIP Conference Proceedings 208, New York, 1990, pp 96-105.
3. Skinner, K.A., and Stalker, R.J. "A Time-of-Flight Mass Spectrometer for Impulse Facilities" AIAA Journal, Vol 32, No 11, 1994, pp 2325-2328.
4. Lordi, J.A., Mates, R.E., & Moselle, J.R., "Computer Program for the Numerical Solution of Non-Equilibrium Expansions of Reacting Gas Mixtures", NASA CR-472, May 1966.
5. Krishnakumar, E., & Srivastara, S.K., "Cross-Sections for Electron Impact Ionization of O<sub>2</sub>", Int. J. Mass. Spec. Ion Proc., Vol 113, 1992, pp 1-12.
6. Bell, K.L., Gilbody, H.B., Hughes, J.G., Kingston, A.E. & Smith, F.J. "Recommended Data on the Electron Impact Ionization of Light Atoms and Ions". J. Phys. Chem. Ref. Data Vol 12, 1983, pp 891-916.
7. Krishnakumar, E., & Srivastava, S.K., "Cross-Sections for the Production of N<sub>2</sub><sup>+</sup>, N<sup>+</sup>, N<sub>2</sub><sup>2+</sup> and N<sup>2</sup> by Electron Impact on N<sub>2</sub>", J. Phys. B: At. mol. Opt. Phys., Vol 23, 1990, pp 1893-1903.
8. Rapp, D. & Englander-Golden, P., "Total Cross-Sections for Ionization and Attachment in Gases by Electron Impact. I. Positive Ionization", J. Chem. Phys., Vol 43, 1965, pp 1464-1479.
9. Sagnier, P., & Marraffa, L., "Parametric Study of Thermal and Chemical Nonequilibrium Nozzle Flow" AIAA Journal, Vol 29, No. 3, 1991, pp 334-343.

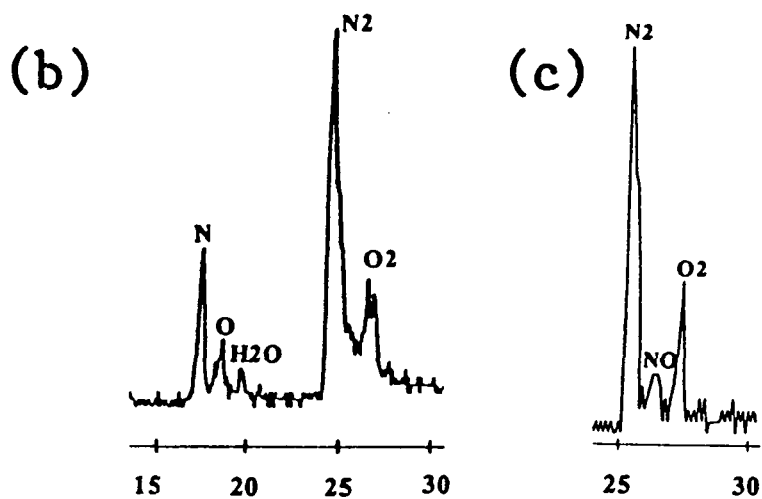
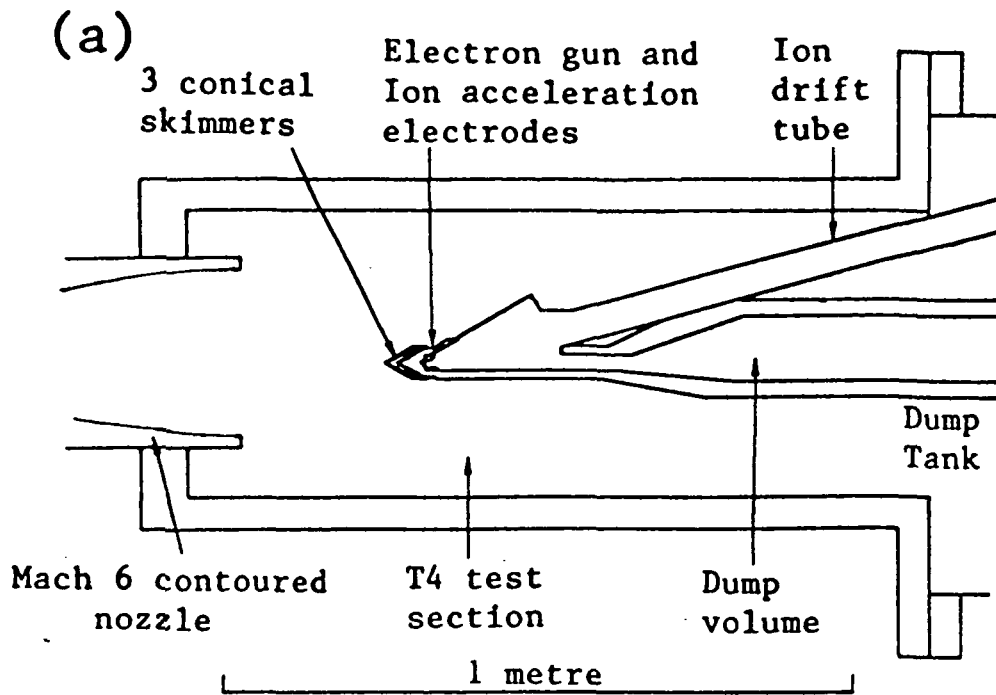
## LIST OF FIGURES

Fig 1. Mass Spectrometer.

- (a) Experimental arrangement
- (b) Typical mass spectrum
- (c) Improved resolution mass spectrum.

Fig 2. Relative Size of Mass Peaks.

- (a) Molecular oxygen Vs molecular nitrogen
- (b) Nitric oxide Vs molecular nitrogen
- (c) Atomic oxygen Vs molecular oxygen.



Time after Electron Gun pulse (microsec)

Fig 1. Mass Spectrometer.

(a) Experimental arrangement

(b) Typical mass spectrum

(c) Improved resolution mass spectrum.

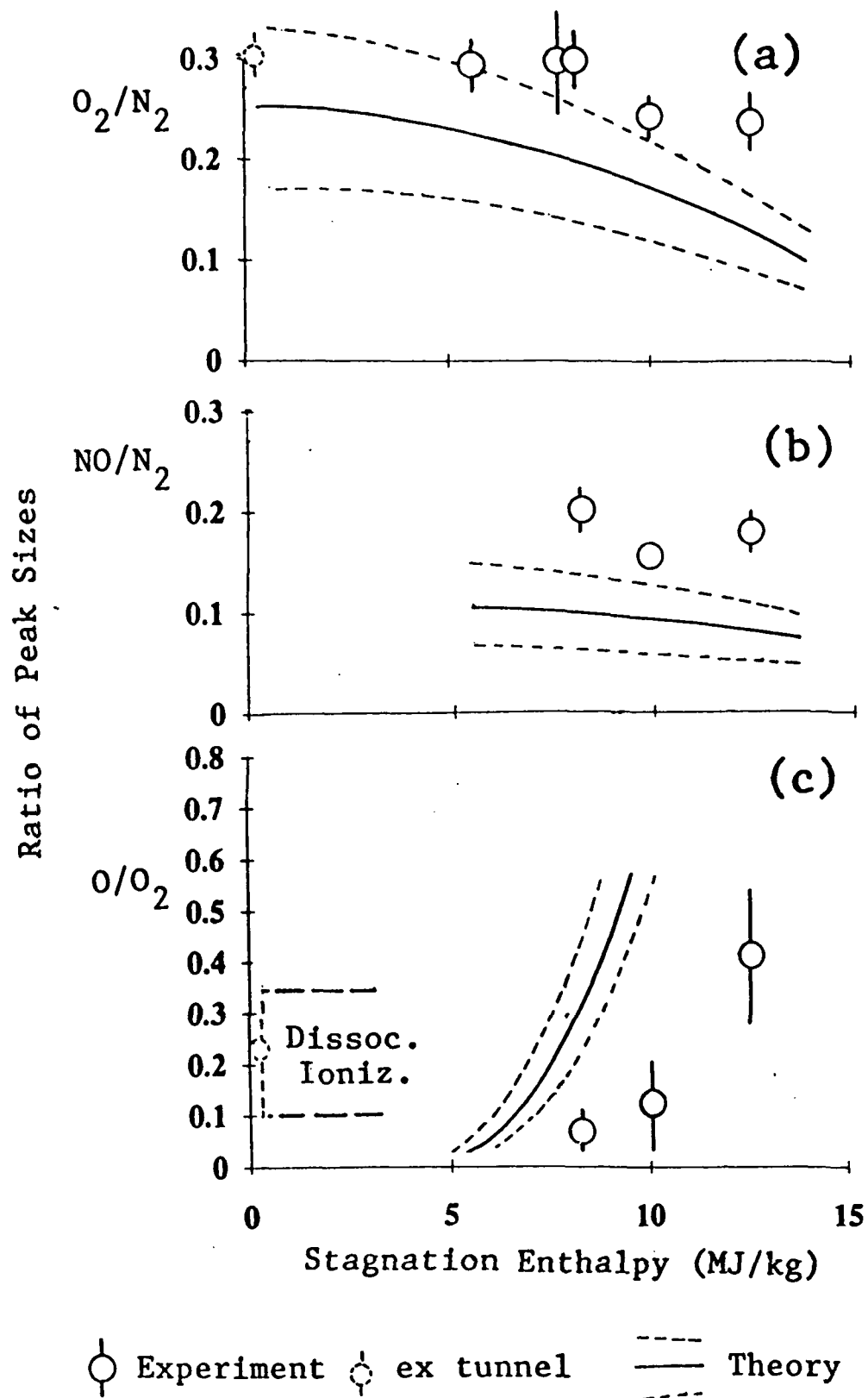


Fig 2. Relative Size of Mass Peaks.

(a) Molecular oxygen Vs molecular nitrogen

(b) Nitric oxide Vs molecular nitrogen

(c) Atomic oxygen Vs molecular oxygen.